1   **Optimization of Non-Coding Regions Improves Protective Efficacy of an**

2   **mRNA SARS-CoV-2 Vaccine in Nonhuman Primates**

3

4   Makda S. Gebre[1*], Susanne Rauch[2*], Nicole Roth[2], Jingyou Yu[1], Abishek Chandrashekar[1], Noe B.

5   Mercado[1], Xuan He[1], Jinyan Liu[1], Katherine McMahan[1], Amanda Martinot[3], Tori Giffin[1], David

6   Hope[1], Shivani Patel[1], Daniel Sellers[1], Owen Sanborn[1], Julia Barrett[1], Xiaowen Liu[5], Andrew C.

7   Cole[5], Laurent Pessaint[5], Daniel Valentin[5], Zack Flinchbaugh[5], Jake Yalley-Ogunro[5], Jeanne

8   Muench[5], Renita Brown[5], Anthony Cook[5], Elyse Teow[5], Hanne Andersen[5], Mark G. Lewis[5],

9   Stefan O. Mueller[2], Benjamin Petsch[*2], Dan H. Barouch[*,1,6]

10

11   [1]Center for Virology and Vaccine Research, Beth Israel Deaconess Medical Center, Harvard

12   Medical School, Boston, MA 02215, USA; [2]CureVac AG, Tübingen, Germany; [3]Tufts

13   University Cummings School of Veterinary Medicine, North Grafton, MA, USA; [4]Department

14   of Emergency Medicine, Beth Israel Deaconess Medical Center, Boston, MA 02215, USA;

15   [5]Bioqual, Rockville, MD 20852, USA; [6]Ragon Institute of MGH, MIT and Harvard, Cambridge,

16   MA, USA

17

18   Corresponding Authors: Dan H. Barouch (dbarouch@bidmc.harvard.edu); Susanne Rauch

19   (Susanne.rauch@curevac.com)

20

21   * These authors contributed equally to the study

22

23   **The CVnCoV (CureVac) mRNA vaccine for SARS-CoV-2 has recently been evaluated in a**

24   **phase 2b/3 efficacy trial in humans. CV2CoV is a second-generation mRNA vaccine with**

25   **optimized non-coding regions and enhanced antigen expression. Here we report a head-to-**

26   **head study of the immunogenicity and protective efficacy of CVnCoV and CV2CoV in**

27   **nonhuman primates. We immunized 18 cynomolgus macaques with two doses of 12 ug of**

28   **lipid nanoparticle formulated CVnCoV, CV2CoV, or sham (N=6/group). CV2CoV induced**

29   **substantially higher binding and neutralizing antibodies, memory B cell responses, and T cell**

30   **responses as compared with CVnCoV. CV2CoV also induced more potent neutralizing**

31   **antibody responses against SARS-CoV-2 variants, including B.1.351 (beta), B.1.617.2 (delta),**

32   **and C.37 (lambda). While CVnCoV provided partial protection against SARS-CoV-2 challenge,**

33   **CV2CoV afforded robust protection with markedly lower viral loads in the upper and lower**

34   **respiratory tract. Antibody responses correlated with protective efficacy. These data**

35   **demonstrate that optimization of non-coding regions can greatly improve the**

36   **immunogenicity and protective efficacy of an mRNA SARS-CoV-2 vaccine in nonhuman**

37   **primates.**

38   The CVnCoV mRNA vaccine (CureVac) has recently reported efficacy results in humans in

39   the Phase 2b/3 HERALD trial in a population that included multiple viral variants. The observed

40   vaccine efficacy against symptomatic COVID-19 was approximately 48% and 53% in the overall

41   study population and in the 18-60 years of age subgroup, respectively [1]. CV2CoV is a second-

42   generation mRNA vaccine that involves modifications of the non-coding regions that were

43   selected based on an empiric screen for improved antigen expression [2, 3]. Both CVnCoV and

44   CV2CoV are based on RNActive® technology [4-7] that consists of non-chemically modified,

45   sequence engineered mRNA, without pseudouridine [6-12]. Both vaccines encode for the same

46   full-length, pre-fusion stabilized SARS-CoV-2 Spike (S) [13, 14] and are encapsulated in lipid

47   nanoparticles (LNP) with identical composition. CV2CoV has been engineered with different non-

48   coding regions flanking the open reading frame, which have previously been shown to improve

49   transgene expression [3] and protection against SARS-CoV-2 in ACE2 transgenic mice [2].

50   Specifically, CV2CoV includes 5' UTR HSD17B4 and 3' UTR PSMB3 elements, followed by a histone

51   stem loop motif and a poly-A sequence (Fig. 1a; see Methods). In this study, we compare head-

52   to-head the immunogenicity and protective efficacy of CVnCoV and CV2CoV against SARS-CoV-2

53   challenge in nonhuman primates.

54

55   **Vaccine Immunogenicity**

56   We immunized 18 cynomolgus macaques intramuscularly with either 12 μg CVnCoV or

57   CV2CoV or sham vaccine (Fig. 1b). Animals were primed at week 0 and boosted at week 4. Sera

58   was isolated from all animals 24h after the first vaccination to assess innate cytokine responses.

59   CV2CoV induced higher levels of IFNα2a, IP-10 and MIP-1 compared with CVnCoV (P = 0.0152, P

60   = 0.0152, P = 0.0411, respectively; Extended Data Fig. 1).

61   Binding antibody responses were assessed by receptor binding domain (RBD)-specific

62   ELISAs at multiple timepoints following immunization [15, 16]. At week 2, binding antibody titers

63   were only detected with CV2CoV and not with CVnCoV (CVnCoV median titer 25 [range 25-25];

64   CV2CoV median titer 799 [range 82-2,010]) (Fig. 2a). One week following the week 4 boost,

65   antibody titers increased in both groups (CVnCoV median titer 48 [range 75-710]); CV2CoV

66   median titer 28,407 [range 2,714-86,541]) (Fig. 2a). By week 8, binding antibody titers increased

67   in the CVnCoV group but were still >50-fold lower than in the CV2CoV group (P=0.0043) (CVnCoV

68   median titer 214 [range 47-1,238]; CV2CoV median titer 14,827 [range 2,133-37,079]).

69   Neutralizing antibody (NAb) responses were assessed by pseudovirus neutralization

70   assays initially using the vaccine-matched SARS-CoV-2 wildtype (WT) WA1/2020 strain [15-17].

71   NAb titers followed a similar trend as binding antibody titers (Fig. 2b). At week 2, NAb were only

72   detected with CV2CoV and not with CVnCoV (CVnCoV median titer 20 [range 20-20]; CV2CoV

73   median titer 131 [range 62-578]) (Fig. 2b). One week following the week 4 boost, NAb titers

74   increased (CVnCoV median titer 55 [range 20-302]; CV2CoV median titer 2,758 [range 583-

75   11,941]). By week 8, NAb titers increased in the CVnCoV group but were still >10-fold lower than

76   in the CV2CoV group (P=0.0043) (CVnCoV median titer 83 [range 20-335]; CV2CoV median titer

77   991 [range 253-2,765]).

78   At week 6, median NAb titers against the WT WA1/2020, D614G, B.1.1.7 (alpha), and

79   B.1.351 (beta) variants were 456, 121, 101, and 189, respectively, for CVnCoV and were 12,181,

80   4962, 1813, and 755, respectively, for CV2CoV (Fig. 2c). Median NAb titers against C.37 (lamda),

81   B.1.617.1 (kappa), and B.1.617.2 (delta) were 516, 158, and 36, respectively, for CVnCoV and

82   were 1195, 541, and 568, respectively, for CV2CoV (Extended Data Fig. 2). Taken together, these

83   data show that CV2CoV induced substantially higher NAb titers as well against SARS-CoV-2

84   variants compared with CVnCoV.

85   Most SARS-CoV-2 RBD-specific B cells reside within the memory B cell pool [18]. We

86   assessed memory B cell responses in blood from CVnCoV, CV2CoV and sham vaccinated NHPs by

87   flow cytometry [19]. RBD- and Spike-specific memory B cells were detected in the CV2CoV group,

88   but not in the CVnCoV group at week 6 (Fig. 3a, 3b). The cells were not detected at week 1 for

89   both groups (data not shown). T cell responses were assessed by IFN-γ enzyme-linked

90   immunosorbent spot (ELISPOT) assay using pooled S peptides at week 6 in both groups but were

91   higher in the CV2CoV group (P=0.0065) (Fig. 3c).

92

93   **Protective Efficacy**

94   All animals were challenged at week 8 with 1.0×10^5 $TCID_{50}$ SARS-CoV-2 WA1/2020 via the

95   intranasal (IN) and intratracheal (IT) routes. Viral loads were assessed in bronchoalveolar lavage

96   (BAL) and nasal swab (NS) samples collected on days 1, 2, 4, 7 and 10 following challenge by RT-

97   PCR specific for subgenomic mRNA (sgRNA) [20]. High subgenomic RNA levels were observed in

98   BAL and NS in the sham group peak on day 2 and largely resolved by day 10. Sham controls had

99   a peak median of 6.02 (range 4.62–6.81) $\log_{10}$ sgRNA copies/ml in BAL and 7.35 (range 5.84–8.09)

100   $\log_{10}$ sgRNA copies/swab in NS on day 2 (Fig. 4). CVnCoV immunized animals showed a peak

101   median of 4.92 (range 2.40–6.61) $\log_{10}$ sgRNA copies/ml in BAL and 6.42 (range 4.46–7.81) $\log_{10}$

102   sgRNA copies/swab in NS (Fig. 4). CV2CoV immunized animals exhibited a peak median of 2.90

103   (range 1.70–4.64) $\log_{10}$ sgRNA copies/ml in BAL and 3.17 (range 2.59–5.63) $\log_{10}$ sgRNA

104   copies/swab in NS (Fig. 4), with resolution of sgRNA in BAL by day 2 in most animals and by day

105   4 in all animals. Overall, CV2CoV resulted in significantly lower peak viral loads than CVnCoV in

106   both BAL (P=0.0411) and NS (P=0.0087) (Fig. 5a and b).

107   We next evaluated immune correlates of protection in this study. The $\log_{10}$ ELISA and NAb

108   titers at week 6 inversely correlated with peak $\log_{10}$ sgRNA copies/ml in BAL (P=0.0008,

109   R=−0.7148 and P=0.0015, R= −0.6912, respectively, two-sided Spearman rank-correlation test)

110   (Fig. 5, c and e) and with peak sgRNA copies/nasal swab in NS (P<0.0001, R=−0.8346, and

111   P<0.0001, R=−0.8766, respectively, two-sided Spearman rank-correlation test) (Fig. 5, d and f).

112   Consistent with prior observations from our laboratory and others [15, 16, 21], these findings

113   suggest that binding and neutralizing antibody titers are important correlates of protection for

114   these SARS-CoV-2 vaccines in nonhuman primates.   Similar correlates of protection were

115   observed with viral loads assessed as area under the curve (AUC) (Extended Data Fig. 3).

116   Following challenge, we observed anamnestic binding and neutralizing antibody

117   responses in the CVnCoV vaccinated animals (Extended Data Fig. 4). We did not observe higher

118   antibody responses in the CV2CoV vaccinated animals following challenge, likely reflecting the

119   robust protection and minimal viral replication in these animals, as we have previously reported

120   [16].

121   On day 10 post-challenge, animals were necropsied, and lung tissues were evaluated by

122   histopathology. Although viral replication had largely resolved by this timepoint, sham animals

123   had higher cumulative lung pathology scores [19] as compared to both CVnCoV and CV2CoV

124   vaccinated animals (CVnCoV P= 0.0368; CV2CoV P= 0.0022) (Extended Data Fig. 5a). Sham

125   animals also had more lung lobes affected (Extended Data Fig. 5b) and more extensive lung

126   lesions with a greater proportion of lung lobes showing evidence of interstitial inflammation,

127   alveolar inflammatory infiltrates, and type II pneumocyte hyperplasia (Extended Data Fig. 5c-h).

128   No significant differences were observed between the cumulative lung scores between CVnCoV

129   and CV2CoV vaccinated animals on day 10. Pathologic lesions in vaccinated animals were similar

130   to those observed in sham animals (Extended Data Fig. 5i-l) but fewer overall and more focal in

131   distribution.

132

Discussion

134   CV2CoV elicited substantially higher humoral and cellular immune responses and

135   provided significantly improved protective efficacy against SARS-CoV-2 challenge compared with

136   CVnCoV in macaques. These data suggest that optimization of non-coding elements of the mRNA

137   backbone can substantially improve the immunogenicity and protective efficacy of mRNA

138   vaccines. Both CVnCoV and CV2CoV contain non-modified nucleotides, without pseudouridine

139   or derivates, and CV2CoV has previously been shown to lead to higher antigen expression than

140   CVnCoV in cell culture [3]. While previous studies in rodents and nonhuman primates have

141   demonstrated protection by CVnCoV [2, 22][23] this was only studied in the lower respiratory

142   tract [22][23]. In the present study, CVnCoV provided only modest reductions in viral loads in

143   BAL and NS compared with sham controls. In contrast, CV2CoV induced >10-fold higher NAb

144   responses than CVnCoV against multiple viral variants and provided >3 log reductions in sgRNA

145   copies/ml in BAL and >4 log reductions in sgRNA copies/swab in NS compared with sham controls.

146   Previous mRNA vaccine clinical trials have demonstrated onset of protective efficacy after

147   the first dose and improved protection after the boost immunization [24, 25]. In the present

148   study, the prime immunization with CV2CoV induced binding and neutralizing antibodies in all

149   macaques by week 2, and these responses increased substantially by 1 week after the boost

150   immunization. Although comparisons with other nonhuman primate studies are difficult due to

151   differences in study designs and laboratory assays, NAb titers induced by CV2CoV appear roughly

152   similar to those reported for previous mRNA vaccines in macaques [26, 27].

153   As previously reported for other vaccines [28-32], NAb titers were lower to certain SARS-

154   CoV-2 variants, including B.1.351 (beta) and B.1.617.2 (delta), than to the parental strain

155   WA1/2020. Although our challenge virus in this study was SARS-CoV-2 WA1/2020, NAb titers

156   elicited by CV2CoV to these viral variants exceeded the threshold that we previously reported as

157   threshold titers for protection (50-100) [17, 19, 21]. However, future studies will be required to

158   assess directly the protective efficacy of CV2CoV against SARS-CoV-2 variants of concern in non-

159   human primates.

160   CV2CoV induced both antigen-specific memory B cell responses and T cell responses.

161   While the correlates of protection in this study were binding and neutralizing antibodies [33, 34],

162   it is likely that $CD8^+$ T cells contribute to viral clearance in tissues [35, 36]. We previously reported

163   that depletion of $CD8^+$ T cells partially abrogated protective efficacy against SARS-CoV-2 re-

164   challenge in convalescent macaques [21]. Memory B cells may contribute to durability of

165   antibody responses [37, 38], although B cell germinal center responses and durability of

166   protective efficacy following CV2CoV vaccination remain to be determined. Moreover, although

167   this study was not specifically designed as a safety study, it is worth noting that we did not

168   observe any adverse effects following CVnCoV or CV2CoV vaccination, and we did not observe

169   any unexpected or enhanced pathology in the vaccinated animals at necropsy [39].

170   In summary, our data show that optimization of non-coding regions in a SARS-CoV-2

171   mRNA vaccine can substantially improve its immunogenicity against multiple viral variants and

172   enhance protective efficacy against SARS-CoV-2 challenge in nonhuman primates. Improved

173   characteristics of CV2CoV, compared with CVnCoV, could translate into increased efficacy in

174   humans, and clinical trials of CV2CoV are planned.

175

189   **Author contributions:** S.R., B.P., S.O.M., N.R. and D.H.B. designed the study. M.S.G., J.Y., A.C., N.

190   M., X. H., J. L., K. M., A. M., T.G., D.H., S.P., D.S., O.S., and J.B. performed immunologic and

191   virologic assays. X.L. and A.C.C. performed cytokine analysis. L.P., D.V., Z.F., J.Y., J.M., R.B., A.C.,

192   E.T., H.A. and M.L. led the clinical care of the animals. M.S.G. and D.H.B. wrote the paper with all

193   coauthors.

194   **Competing interests:** S.R., B.P., N.R., and S.O.M. are employees of CureVac AG, Tübingen,

195   Germany, a publicly listed company developing mRNA-based vaccines and immunotherapeutics.

196   Authors may hold shares in the company. S.R. and B.P. and N.R. are inventors on several patents

197   on mRNA vaccination and use thereof. The other authors declare no competing interests.

198   **Corresponding authors:** Dan H. Barouch, M.D.; Email: dbarouch@bidmc.harvard.edu; Susanne

199   Rauch, Ph.D., Email: Susanne.rauch@curevac.com

200

References

1. AG, C., *CureVac Final Data from Phase 2b/3 Trial of First-Generation COVID-19 Vaccine Candidate, CVnCoV, Demonstrates Protection in Age Group of 18 to 60* https://www.curevac.com/en/2021/06/30/curevac-final-data-from-phase-2b-3-trial-of-first-generation-covid-19-vaccine-candidate-cvncov-demonstrates-protection-in-age-group-of-18-to-60/.

2. Hoffmann, D., et al., *CVnCoV and CV2CoV protect human ACE2 transgenic mice from ancestral B BavPat1 and emerging B.1.351 SARS-CoV-2.* Nat Commun, 2021. **12**(1): p. 4048.

3. Nicole Roth, J.S., Donata Hoffmann, Moritz Thran, Andreas Thess, Stefan O. Mueller, Benjamin Petsch and Susanne Rauch, *CV2CoV, an enhanced mRNA-based SARS-CoV-2 vaccine candidate, supports higher protein expression and improved immunogenicity in rats.* bioRxiv, 2021.

4. Hoerr, I., et al., *In vivo application of RNA leads to induction of specific cytotoxic T lymphocytes and antibodies.* Eur J Immunol, 2000. **30**(1): p. 1-7.

5. Fotin-Mleczek, M., et al., *Highly potent mRNA based cancer vaccines represent an attractive platform for combination therapies supporting an improved therapeutic effect.* J Gene Med, 2012. **14**(6): p. 428-39.

6. Fotin-Mleczek, M., et al., *Messenger RNA-based vaccines with dual activity induce balanced TLR-7 dependent adaptive immune responses and provide antitumor activity.* J Immunother, 2011. **34**(1): p. 1-15.

7. Kubler, H., et al., *Self-adjuvanted mRNA vaccination in advanced prostate cancer patients: a first-in-man phase I/IIa study.* J Immunother Cancer, 2015. **3**: p. 26.

8. Lutz, J., et al., *Unmodified mRNA in LNPs constitutes a competitive technology for prophylactic vaccines.* NPJ Vaccines, 2017. **2**: p. 29.

9. Stitz, L., et al., *A thermostable messenger RNA based vaccine against rabies.* PLoS Negl Trop Dis, 2017. **11**(12): p. e0006108.

10. Schnee, M., et al., *An mRNA Vaccine Encoding Rabies Virus Glycoprotein Induces Protection against Lethal Infection in Mice and Correlates of Protection in Adult and Newborn Pigs.* PLoS Negl Trop Dis, 2016. **10**(6): p. e0004746.

11. Petsch, B., et al., *Protective efficacy of in vitro synthesized, specific mRNA vaccines against influenza A virus infection.* Nat Biotechnol, 2012. **30**(12): p. 1210-6.

12. Aldrich, C., et al., *Proof-of-concept of a low-dose unmodified mRNA-based rabies vaccine formulated with lipid nanoparticles in human volunteers: A phase 1 trial.* Vaccine, 2021. **39**(8): p. 1310-1318.

13. Pallesen, J., et al., *Immunogenicity and structures of a rationally designed prefusion MERS-CoV spike antigen.* Proc Natl Acad Sci U S A, 2017. **114**(35): p. E7348-E7357.

14. Kirchdoerfer, R.N., et al., *Stabilized coronavirus spikes are resistant to conformational changes induced by receptor recognition or proteolysis.* Sci Rep, 2018. **8**(1): p. 15701.

15. Yu, J., et al., *DNA vaccine protection against SARS-CoV-2 in rhesus macaques.* Science, 2020. **369**(6505): p. 806-811.

16. Mercado, N.B., et al., *Single-shot Ad26 vaccine protects against SARS-CoV-2 in rhesus macaques.* Nature, 2020. **586**(7830): p. 583-588.

244   17.   Chandrashekar, A., et al., *SARS-CoV-2 infection protects against rechallenge in rhesus*
245   *macaques.* Science, 2020. **369**(6505): p. 812-817.

246   18.   He, X., et al., *Low-Dose Ad26.COV2.S Protection Against SARS-CoV-2 Challenge in Rhesus*
247   *Macaques.* Cell, 2021.

248   19.   He, X., et al., *Low-dose Ad26.COV2.S protection against SARS-CoV-2 challenge in rhesus*
249   *macaques.* Cell, 2021. **184**(13): p. 3467-3473 e11.

250   20.   Dagotto, G., et al., *Comparison of Subgenomic and Total RNA in SARS-CoV-2 Challenged*
251   *Rhesus Macaques.* J Virol, 2021.

252   21.   McMahan, K., et al., *Correlates of protection against SARS-CoV-2 in rhesus macaques.*
253   Nature, 2021. **590**(7847): p. 630-634.

254   22.   Rauch, S., et al., *mRNA-based SARS-CoV-2 vaccine candidate CVnCoV induces high levels*
255   *of virus-neutralising antibodies and mediates protection in rodents.* NPJ Vaccines, 2021.
256   **6**(1): p. 57.

257   23.   Susanne Rauch, K.G., Yper Hall, Francisco J. Salguero, Mike J. Dennis, Fergus V. Gleeson,
258   Debbie Harris, Catherine Ho, Holly E. Humphries, Stephanie Longet, Didier Ngabo,
259   Jemma Paterson, Emma L. Rayner , Kathryn A. Ryan, Sally Sharpe, Robert J. Watson,
260   Stefan O. Mueller, Benjamin Petsch, Miles W. Carroll *mRNA vaccine CVnCoV protects*
261   *non-human primates from SARS-CoV-2 challenge infection.* bioRxiv, 2020.

262   24.   Polack, F.P., et al., *Safety and Efficacy of the BNT162b2 mRNA Covid-19 Vaccine.* N Engl J
263   Med, 2020. **383**(27): p. 2603-2615.

264   25.   Baden, L.R., et al., *Efficacy and Safety of the mRNA-1273 SARS-CoV-2 Vaccine.* N Engl J
265   Med, 2021. **384**(5): p. 403-416.

266   26.   Corbett, K.S., et al., *Evaluation of the mRNA-1273 Vaccine against SARS-CoV-2 in*
267   *Nonhuman Primates.* N Engl J Med, 2020. **383**(16): p. 1544-1555.

268   27.   Vogel, A.B., et al., *BNT162b vaccines protect rhesus macaques from SARS-CoV-2.* Nature,
269   2021. **592**(7853): p. 283-289.

270   28.   Liu, C., et al., *Reduced neutralization of SARS-CoV-2 B.1.617 by vaccine and convalescent*
271   *serum.* Cell, 2021.

272   29.   Haas, E.J., et al., *Impact and effectiveness of mRNA BNT162b2 vaccine against SARS-*
273   *CoV-2 infections and COVID-19 cases, hospitalisations, and deaths following a*
274   *nationwide vaccination campaign in Israel: an observational study using national*
275   *surveillance data.* Lancet, 2021. **397**(10287): p. 1819-1829.

276   30.   Wu, K., et al., *Serum Neutralizing Activity Elicited by mRNA-1273 Vaccine.* N Engl J Med,
277   2021. **384**(15): p. 1468-1470.

278   31.   Wibmer, C.K., et al., *SARS-CoV-2 501Y.V2 escapes neutralization by South African COVID-*
279   *19 donor plasma.* Nat Med, 2021. **27**(4): p. 622-625.

280   32.   Wall, E.C., et al., *Neutralising antibody activity against SARS-CoV-2 VOCs B.1.617.2 and*
281   *B.1.351 by BNT162b2 vaccination.* Lancet, 2021. **397**(10292): p. 2331-2333.

282   33.   Philipp, M. and G. Santibanez, *Preference of respiratory phases to perform reaction time*
283   *tasks.* Act Nerv Super (Praha), 1988. **30**(2): p. 153-5.

284   34.   Feng, S., et al., *Correlates of protection against symptomatic and asymptomatic SARS-*
285   *CoV-2 infection.* medRxiv, 2021: p. 2021.06.21.21258528.

286   35.   Lafon, E., et al., *Potent SARS-CoV-2-Specific T Cell Immunity and Low Anaphylatoxin*
287   *Levels Correlate With Mild Disease Progression in COVID-19 Patients.* Front Immunol,
288   2021. **12**: p. 684014.
289   36.   Schmidt, M.E. and S.M. Varga, *The CD8 T Cell Response to Respiratory Virus Infections.*
290   Front Immunol, 2018. **9**: p. 678.
291   37.   Abayasingam, A., et al., *Long-term persistence of RBD(+) memory B cells encoding*
292   *neutralizing antibodies in SARS-CoV-2 infection.* Cell Rep Med, 2021. **2**(4): p. 100228.
293   38.   Dan, J.M., et al., *Immunological memory to SARS-CoV-2 assessed for up to 8 months*
294   *after infection.* Science, 2021. **371**(6529).
295   39.   Graham, B.S., *Rapid COVID-19 vaccine development.* Science, 2020. **368**(6494): p. 945-
296   946.
297   40.   Yu, J., et al., *Deletion of the SARS-CoV-2 Spike Cytoplasmic Tail Increases Infectivity in*
298   *Pseudovirus Neutralization Assays.* J Virol, 2021.
299   41.   Wolfel, R., et al., *Virological assessment of hospitalized patients with COVID-2019.*
300   Nature, 2020. **581**(7809): p. 465-469.
301
302

Materials and Methods

mRNA vaccines

The two mRNA vaccines, CVnCoV and CV2CoV, are based on CureVac's RNActive® platform (claimed and described in e.g. WO2002098443 and WO2012019780) and do not include chemically modified nucleosides. They are comprised of a 5' cap1 structure, a GC-enriched open reading frame (ORF), 3' UTR and a vector-encoded poly-A stretch. CVnCoV contains a cleanCap (Trilink), parts of the 3' UTR of the Homo sapiens alpha haemoglobin gene as 3' UTR, followed by a poly-A (64) stretch, a polyC (30) stretch and a histone stem loop [22, 23]. CV2CoV has previously been described to contain a cleanCap followed by 5' UTR from the human hydroxysteroid 17-beta dehydrogenase 4 gene (HSD17B4) and a 3' UTR from human proteasome 20S subunit beta 3 gene (PSMB3), followed by a histone stem loop and a poly-A (100) stretch [3]. Both constructs were encapsulated in lipid nanoparticles (LNP) by Acuitas Therapeutics (Vancouver, Canada) (CV2CoV) or Polymun Scientific Immunbiologische Forschung GmbH (Klosterneuburg, Austria) (CVnCoV). LNPs are composed of ionizable amino lipid, phospholipid, cholesterol, and a PEGylated lipid; compositions for CVnCoV and CV2CoV are identical. Both mRNAs encode for SARS-CoV-2 full length spike protein containing stabilizing K986P and V987P mutations (NCBI Reference Sequence NC_045512.2).

Animals and study design

18 cynomolgus macaques were randomly assigned to three groups. Animals received either CVnCoV (N=6) or CV2CoV (N=6) mRNA vaccines or were designated as sham controls (N=6). The mRNA vaccines were administered at a 12 µg dose, intramuscularly, in the left quadriceps on

325   day 0. Boost immunizations were similarly administered at week 4. At week 8, all animals were

326   challenged with 1.0×10^5 TCID$_{50}$ SARS-CoV-2 derived from USA-WA1/2020 (NR-52281; BEI

327   Resources) [17]. Challenge virus was administered as 1 ml by the intranasal (IN) route (0.5 ml in

328   each nare) and 1 ml by the intratracheal (IT) route. All animals were sacrificed 10 days post

329   challenge. Immunologic and virologic assays were performed blinded. All animals were housed

330   at Bioqual, Inc. (Rockville, MD). All animal studies were conducted in compliance with all relevant

331   local, state, and federal regulations and were approved by the Bioqual Institutional Animal Care

332   and Use Committee (IACUC).

333

334   **Cytokine analyses**

335   Serum levels of 19 analytes that have been associated with immune response to viral

336   infection were tested using U-PLEX Viral Combo 1 (NHP) kit (K15069L-1) from Meso Scale

337   Discovery (MSD, Rockville, MD). The 19 analytes and their detection limits (LLODs) are G-CSF (1.5

338   pg/mL), GM-CSF (0.12 pg/mL), IFN-α2a (1.7 pg/mL), IFN-γ (1.7 pg/mL), IL-1RA (1.7 pg/mL), IL-1β

339   (0.15 pg/mL), IL-4 (0.06 pg/mL), IL-5 (0.24 pg/mL), IL-6 (0.33 pg/mL), IL-7 (1.5 pg/mL) and IL-8

340   (0.15 pg/mL), IL-9 (0.14 pg/mL), IL-10 (0.14 pg/mL), IL-12p70 (0.54 pg/mL), IP-10 (0.49 pg/mL),

341   MCP-1 (0.74 pg/mL), MIP-1α (7.7 pg/mL), TNF-α (0.54 pg/mL) and VEGF-A (2.0pg/mL). All serum

342   samples were assayed in duplicate. Assay was done by the Metabolism and Mitochondrial

343   Research Core (Beth Israel Deaconess Medical Center, Boston, MA) following manufacture's

344   instruction. The assay plates were read by MESO QUICKPLEX SQ 120 instrument and data were

345   analyzed by DISCOVERY WORKBENCH® 4.0 software.

346

Enzyme-linked immunosorbent assay (ELISA)

RBD-specific binding antibodies were assessed by ELISA as described [16, 17]. Briefly, 96-well plates were coated with 1µg/ml SARS-CoV-2 RBD protein (40592-VNAH, SinoBiological) in 1X DPBS and incubated at 4°C overnight. After incubation, plates were washed once with wash buffer (0.05% Tween 20 in 1 X DPBS) and blocked with 350 µL Casein block/well for 2–3 h at room temperature. After incubation, block solution was discarded, and plates were blotted dry. Serial dilutions of heat-inactivated serum diluted in casein block were added to wells and plates were incubated for 1 h at room temperature. Next, the plates were washed three times and incubated for 1 h with a 1:1000 dilution of anti-macaque IgG HRP (NIH NHP Reagent Program) at room temperature in the dark. Plates were then washed three more times, and 100 µL of SeraCare KPL TMB SureBlue Start solution was added to each well; plate development was halted by the addition of 100 µL SeraCare KPL TMB Stop solution per well. The absorbance at 450nm was recorded using a VersaMax or Omega microplate reader. ELISA endpoint titers were defined as the highest reciprocal serum dilution that yielded an absorbance > 0.2. Log10 endpoint titers are reported. Immunologic assays were performed blinded.

Pseudovirus neutralization assay

The SARS-CoV-2 pseudoviruses expressing a luciferase reporter gene were generated as described previously [15, 40]. Briefly, the packaging plasmid psPAX2 (AIDS Resource and Reagent Program), luciferase reporter plasmid pLenti-CMV Puro-Luc (Addgene), and Spike protein expressing pcDNA3.1-SARS CoV-2 SΔCT of variants were co-transfected into HEK293T cells by lipofectamine 2000 (ThermoFisher). Pseudoviruses of SARS-CoV-2 variants were generated by

17

369   using WA1/2020 strain (Wuhan/WIV04/2019, GISAID accession ID: EPI_ISL_402124), D614G

370   mutation, B.1.1.7 variant (GISAID accession ID: EPI_ISL_601443), B.1.351 variant (GISAID

371   accession ID: EPI_ISL_712096), C37 variant (GenBank ID: QRX62290), B.1.671.1 variant (GISAID

372   accession ID: EPI_ISL_1384866) and B.1.617.2 variant (GISAID accession ID: EPI_ISL_2020950).

373   The supernatants containing the pseudotype viruses were collected 48 h post-transfection, which

374   were purified by centrifugation and filtration with 0.45 μm filter. To determine the neutralization

375   activity of the plasma or serum samples from participants, HEK293T-hACE2 cells were seeded in

376   96-well tissue culture plates at a density of 1.75 x 10^4 cells/well overnight. Three-fold serial

377   dilutions of heat inactivated serum or plasma samples were prepared and mixed with 50 μL of

378   pseudovirus. The mixture was incubated at 37°C for 1 h before adding to HEK293T-hACE2 cells.

379   48 h after infection, cells were lysed in Steady-Glo Luciferase Assay (Promega) according to the

380   manufacturer's instructions. SARS-CoV-2 neutralization titers were defined as the sample dilution

381   at which a 50% reduction in relative light unit (RLU) was observed relative to the average of the

382   virus control wells.

383

384   **B cell immunophenotyping**

385   Fresh PBMCs were stained with Aqua live/dead dye (Invitrogen) for 20 min, washed with

386   2% FBS/DPBS buffer, and suspended in 2% FBS/DPBS buffer with Fc Block (BD) for 10 min,

387   followed by staining with monoclonal antibodies against CD45 (clone D058-1283, BUV805), CD3

388   (clone SP34.2 , APC-Cy7), CD7 (clone M-T701, Alexa700), CD123 (clone 6H6, Alexa700), CD11c

389   (clone 3.9, Alexa700), CD20 (clone 2H7, PE-Cy5), IgA (goat polyclonal antibodies, APC), IgG (clone

390   G18-145, BUV737), IgM (clone G20-127, BUV396), IgD (goat polyclonal antibodies, PE), CD80

391 (clone L307.4, BV786), CD95 (clone DX2, BV711), CD27 (clone M-T271, BUV563), CD21 (clone B-

392 ly4, BV605), CD14 (clone M5E2, BV570) and CD138 (clone DL-101, PE-CF594). Cells were also

393 stained with SARS-CoV-2 antigens including biotinylated SARS-CoV-2 RBD protein (Sino

394 Biological) and full-length SARS-CoV-2 Spike protein (Sino Biological) labeled with FITC and

395 DyLight 405 (DyLight® 405 Conjugation Kit, FITC Conjugation Kit , Abcam), at 4 °C for 30 min. After

396 staining, cells were washed twice with 2% FBS/DPBS buffer, followed by incubation with BV650

397 streptavidin (BD Pharmingen) for 10min, then washed twice with 2% FBS/DPBS buffer. After

398 staining, cells were washed and fixed by 2% paraformaldehyde. All data were acquired on a BD

399 FACSymphony flow cytometer. Subsequent analyses were performed using FlowJo software

400 (Treestar, v.9.9.6). Immunologic assays were performed blinded.

401

402 **IFN-γ enzyme-linked immunospot (ELISPOT) assay**

403   ELISPOT plates were coated with mouse anti-human IFN-γ monoclonal antibody from BD

404 Pharmingen at a concentration of 5 µg/well overnight at 4°C. Plates were washed with DPBS

405 containing 0.25% Tween 20, and blocked with R10 media (RPMI with 11% FBS and 1.1% penicillin-

406 streptomycin) for 1 h at 37°C. The Spike 1 and Spike 2 peptide pools (JPT Peptide Technologies,

407 custom made) used in the assay contain 15 amino acid peptides overlapping by 11 amino acids

408 that span the protein sequence and reflect the N- and C- terminal halves of the protein,

409 respectively. Spike 1 and Spike 2 peptide pools were prepared at a concentration of 2 µg/well,

410 and 200,000 cells/well were added. The peptides and cells were incubated for 18–24 h at 37°C.

411 All steps following this incubation were performed at room temperature. The plates were washed

412 with ELISPOT wash buffer and incubated for 2 h with Rabbit polyclonal anti-human IFN-γ Biotin

413   from U-Cytech (1 μg/mL). The plates are washed a second time and incubated for 2 h with

414   Streptavidin-alkaline phosphatase antibody from Southern Biotechnology (1 μg/mL). The final

415   wash was followed by the addition of Nitro-blue Tetrazolium Chloride/5-bromo-4-chloro 3

416   'indolyl phosphate p-toludine salt (NBT/BCIP chromagen) substrate solution (Thermo Scientific)

417   for 7 min. The chromagen was discarded and the plates were washed with water and dried in a

418   dim place for 24 h. Plates were scanned and counted on a Cellular Technologies Limited

419   Immunospot Analyzer.

420

421   **Subgenomic RT-PCR assay**

422   SARS-CoV-2 E gene subgenomic RNA (sgRNA) was assessed by RT-PCR using primers and

423   probes as previously described [15, 17]. A standard was generated by first synthesizing a gene

424   fragment of the subgenomic E gene [41]. The gene fragment was subsequently cloned into a

425   pcDNA3.1+ expression plasmid using restriction site cloning (Integrated DNA Technologies). The

426   insert was *in vitro* transcribed to RNA using the AmpliCap-Max T7 High Yield Message Maker Kit

427   (CellScript). Log dilutions of the standard were prepared for RT-PCR assays ranging from 1×10^{10}

428   copies to 1×10^{-1} copies. Viral loads were quantified from bronchoalveolar lavage (BAL) fluid and

429   nasal swabs (NS). RNA extraction was performed on a QIAcube HT using the IndiSpin QIAcube HT

430   Pathogen Kit according to manufacturer's specifications (Qiagen). The standard dilutions and

431   extracted RNA samples were reverse transcribed using SuperScript VILO Master Mix (Invitrogen)

432   following the cycling conditions described by the manufacturer. A Taqman custom gene

433   expression assay (Thermo Fisher Scientific) was designed using the sequences targeting the E

434   gene sgRNA [41]. The sequences for the custom assay were as follows, forward primer,

435   sgLeadCoV2.Fwd: CGATCTCTTGTAGATCTGTTCTC, E_Sarbeco_R: ATATTGCAGCAGTACGCACACA,

436   E_Sarbeco_P1 (probe): VIC-ACACTAGCCATCCTTACTGCGCTTCG-MGBNFQ. Reactions were carried

437   out in duplicate for samples and standards on the QuantStudio 6 and 7 Flex Real-Time PCR

438   Systems (Applied Biosystems) with the thermal cycling conditions: initial denaturation at 95°C for

439   20 seconds, then 45 cycles of 95°C for 1 second and 60°C for 20 seconds. Standard curves were

440   used to calculate subgenomic RNA copies per ml or per swab. The quantitative assay sensitivity

441   was determined as 50 copies per ml or per swab.

442

443   **Histopathology**

444   At time of fixation, lungs were suffused with 10% formalin to expand the alveoli. All

445   tissues were fixed in 10% formalin and blocks sectioned at 5 μm. Slides were baked for 30-60 min

446   at 65 degrees, deparaffinized in xylene, rehydrated through a series of graded ethanol to distilled

447   water, then stained with hematoxylin and eosin (H&E). Blinded histopathological evaluation was

448   performed by a board-certified veterinary pathologist (AJM).

449

450   **Statistical analyses**

451   Statistical analyses were performed using GraphPad Prism (version 9.0) software

452   (GraphPad Software) and comparison between groups was performed using a two-tailed

453   nonparametric Mann-Whitney U t test. P-values of less than 0.05 were considered significant.

454   Correlations were assessed by two-sided Spearman rank-correlation tests.

455

Figure Legends

Figure 1. (a) mRNA vaccine design and (b) NHP vaccine study schema

Figure 2. CV2CoV elicits high levels of binding and neutralizing antibody responses in NHPs. NHPs (6/group) were vaccinated twice with 12µg of CVnCoV or CV2CoV on d0 and d28 or remained untreated as negative controls (sham). (**a**) Titers of RBD binding antibodies and (**b**) pseudovirus neutralizing antibodies against ancestral SARS-CoV-2 strain were evaluated at different time points post first (week 0, 1, 2 and 4) and second (week 5, 6 and 8) vaccinations. (**c**) Sera isolated on d42 (week 6) were analyzed for pseudovirus neutralizing antibodies titers against the ancestral WA/2020 (WT) strain, virus featuring the D614G mutation, and variants including B.1.1.7 (Alpha) and B.1.351 (Beta). Each dot represents an individual animal, bars depict the median and the dotted line shows limit of detection.

Figure 3. CV2CoV induces memory B cell and T cell immune responses in on day 42. PBMCs from negative control (sham), CVnCoV or CV2CoV vaccinated animals isolated on d42 of the experiment were stained for (**a**) RBD and (**b**) Spike-specific activated memory B cells and analyzed by high-parameter flow cytometry. IFNγ responses to pooled spike peptides were analyzed via ELISPOT (**c**). Each dot represents an individual animal, bars depict the median and the dotted line shows limit of detection. PBMC = peripheral blood mononuclear cell; SFC = spot forming cells

478   **Figure 4. CV2CoV protects NHPs from challenge infection.** Negative control (sham) or animals

479   vaccinated on d0 and d28 of the experiment with 12μg of CVnCoV or CV2CoV as indicated were

480   subjected to challenge infection using 1.0×10^5 $TCID_{50}$ SARS-CoV-2 via intranasal (IN) and

481   intratracheal (IT) routes. BAL (**a**) and nasal swab samples (**b**) collected on days 1, 2, 4, 7 and 10

482   post-challenge were analyzed for levels of replicating virus by RT-PCR specific for subgenomic

483   mRNA (sgRNA). Thin black lines represent an individual animal, thick red lines depict the median

484   and the dotted line shows limit of detection. BAL = bronchoalveolar lavage

485

486   **Figure 5. Titers of binding and neutralizing antibody titers elicited upon CVnCoV and CV2CoV**

487   **vaccination correlate with protection against SARS-CoV-2.** Summary of peak viral loads

488   following SARS-CoV-2 challenge in BAL and Nasal Swab (left panels **a** and **b**); antibody correlates

489   of protection for binding antibodies (middle panels in **c** and **d**) and neutralizing antibodies (right

490   panels **e** and **f**). NAbs = neutralizing antibodies, BAL = bronchoalveolar lavage NS = nasal swab

491

492

493

494   **Extended Data Figure Legends**

495

496   **Extended Data Figure. 1. mRNA vaccination leads to innate cytokine induction in the serum of**

497   **NHPs 24h post immunization.** Sera isolated 24h post first injection were analyzed for a panel of

498   19 cytokines associated with viral infection using a U-PLEX Viral Combo kit from Meso Scale

499   Discovery. Changes in cytokine levels above the detection limits were detectable for 9 cytokines.

500   Each dot represents an individual animal, bars depict the median and the dotted line shows limit

501   of detection. Statistical analysis was performed using Mann-Whitney test.

502

503   **Extended Data Figure. 2. CV2CoV elicits high levels of binding and neutralizing antibody**

504   **responses in NHPs.** NHPs (6/group) were vaccinated twice with 12µg of CVnCoV or CV2CoV on

505   d0 and d28 or remained untreated as negative controls (sham). Sera isolated on d42 (week 6)

506   were analyzed for pseudovirus neutralizing antibodies titers against the ancestral WA/2020 (WT)

507   strain, C.37 (Lambda), B.1.617.1 (Kappa) and B.1.617.2 (Delta). Each dot represents an individual

508   animal, bars depict the median and the dotted line shows limit of detection.

509

510   **Extended Data Figure. 3. Titers of binding and neutralizing antibody titers elicited upon CVnCoV**

511   **and CV2CoV vaccination correlate with protection against SARS-CoV-2.** Summary of area under

512   curve (AUC) viral load values following SARS-CoV-2 challenge in BAL and Nasal Swab (left panels

513   **a** and **b**); antibody correlates of protection for binding antibodies (middle panels in **c** and **d**) and

514   neutralizing antibodies (right panels **e** and **f**). NAbs = neutralizing antibodies, BAL =

515   bronchoalveolar lavage NS = nasal swab

516

Extended Data Figure. 4. Post-challenge binding and neutralizing antibody responses of NHPs.
Negative control (sham) or animals vaccinated on d0 and d28 of the experiment with 12µg of
CVnCoV or CV2CoV as indicated were subjected to challenge infection using 1.0×10^5 TCID$_{50}$ SARS-
CoV-2 via intranasal (IN) and intratracheal (IT) routes.). (**a**) Titers of RBD binding antibodies and
(**b**) pseudovirus neutralizing antibodies against ancestral SARS-CoV-2 strain were evaluated
before (week 8) and a week after challenge infection (week 9). Each dot represents an individual
animal, bars depict the median and the dotted line shows limit of detection. NAbs= neutralizing
antibodies

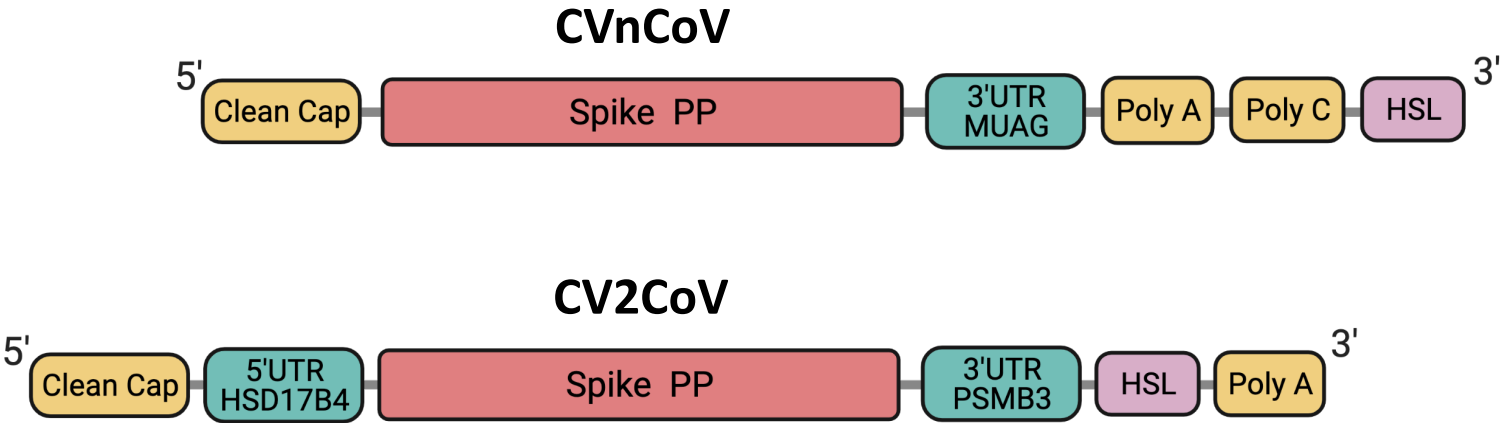**Extended Data Figure. 5: CVnCoV and CV2CoV protect the lungs from pathological changes
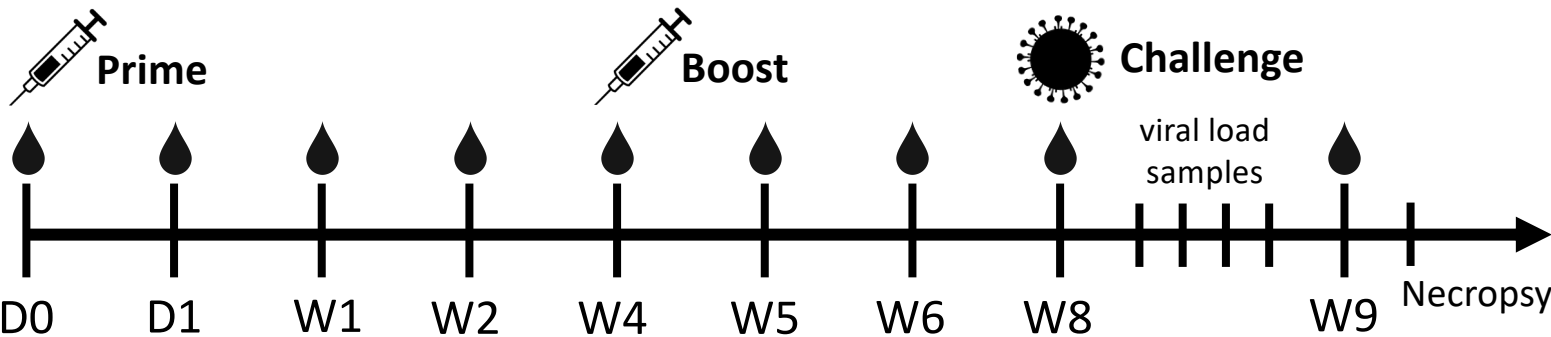upon viral challenge.** Eight lung lobes (4 sections from right and left, caudal to cranial) were
assessed and scored (1-4) for each of the following lesions: 1) Interstitial inflammation and septal
thickening 2) Eosinophilic interstitial infiltrate 3) Neutrophilic interstitial infiltrate 4) Hyaline
membranes 5) Interstitial fibrosis 6) Alveolar infiltrate, macrophage 7) Alveolar/Bronchoalveolar
infiltrate, neutrophils 8) Syncytial cells 9) Type II pneumocyte hyperplasia 10) Broncholar
infiltrate, macrophage 11) Broncholar infiltrate, neutrophils 12) BALT hyperplasia 13)
Bronchiolar/peribronchiolar inflammation 14) Perivascular, mononuclear infiltrates 15) Vessels,
endothelialitis. Each feature assessed was assigned a score of 0= no significant findings;
1=minimal; 2= mild; 3=moderate; 4=marked/severe. (**a**) Cumulative scores per animal (**b**)
Cumulative scores per lung lobe. Individual animals are represented by symbols. Representative
histopathology from sham vaccinated (**c-h**), CnVCoV vaccinated (**i, j**), and Cv2CoV vaccinated (**k,**

538   **l)** animals showing (**c, d,** inset) alveolar macrophage infiltrate, (**e, f,** inset) syncytial cells

539   (arrowheads) and type II pneumocyte hyperplasia, inset (**g, h,** inset) bronchiolar epithelial

540   necrosis with neutrophilic infiltrates (**i**) alveolar neutrophilic infiltrate and alveolar septal

541   thickening (**j**) focal consolidation with inflammation composed of macrophages, neutrophils, and

542   syncytial cells (**k**) focal pneumocyte hyperplasia, syncytial cells and inflammatory infiltrates (**l**)

543   peribronchiolar inflammation. Scale bars: 100 microns (**c**), 50 microns (**e, g**) 20 microns (**i-l**). BALT

544   bronchus associated lymphoid tissue.

a

CVnCoV

5' Clean Cap — Spike PP — 3'UTR MUAG — Poly A — Poly C — HSL 3'

CV2CoV

5' Clean Cap — 5'UTR HSD17B4 — Spike PP — 3'UTR PSMB3 — HSL — Poly A 3'

b

Prime   Boost   Challenge

viral load samples

D0   D1   W1   W2   W4   W5   W6   W8   W9   Necropsy

Groups (N=6)	Vaccines	Antigen	Dose	Route
I	Sham	Sham	Sham	Sham
II	CVnCoV	Full length Spike (K986P, V987P)	12μg	I.M.
III	CV2CoV	Full length Spike (K986P, V987P)	12μg	I.M.

Figure 1

Figure 2

Figure 3

a

BAL

Group I: Sham — $\log_{10}$ sgRNA copies/mL

Group II: CVnCoV — $\log_{10}$ sgRNA copies/mL

Group III: CV2CoV — $\log_{10}$ sgRNA copies/mL

b

Nasal Swab

Group I: Sham — $\log_{10}$ sgRNA copies/swab

Group II: CVnCoV — $\log_{10}$ sgRNA copies/swab

Group III: CV2CoV — $\log_{10}$ sgRNA copies/swab

Figure 4

a

BAL

peak log$_{10}$ sgRNA copies / mL

P = 0.0411

Sham   CVnCoV   CV2CoV

b

Nasal Swab

peak log$_{10}$ sgRNA copies / swab

P = 0.0087

Sham   CVnCoV   CV2CoV

c

ELISA vs BAL

peak log$_{10}$ sgRNA copies / mL

R = -0.7184
P = 0.0008

Wk 6 RBD ELISA titer

d

ELISA vs NS

peak log$_{10}$ sgRNA copies / swab

R = -0.8346
P = <0.0001

Wk 6 RBD ELISA titer

e

Nab vs BAL

peak log$_{10}$ sgRNA copies / mL

R = -0.6912
P = 0.0015

Wk 6 NAb titer

f

NAb vs NS

peak log$_{10}$ sgRNA copies / swab

R = -0.8766
P = <0.0001

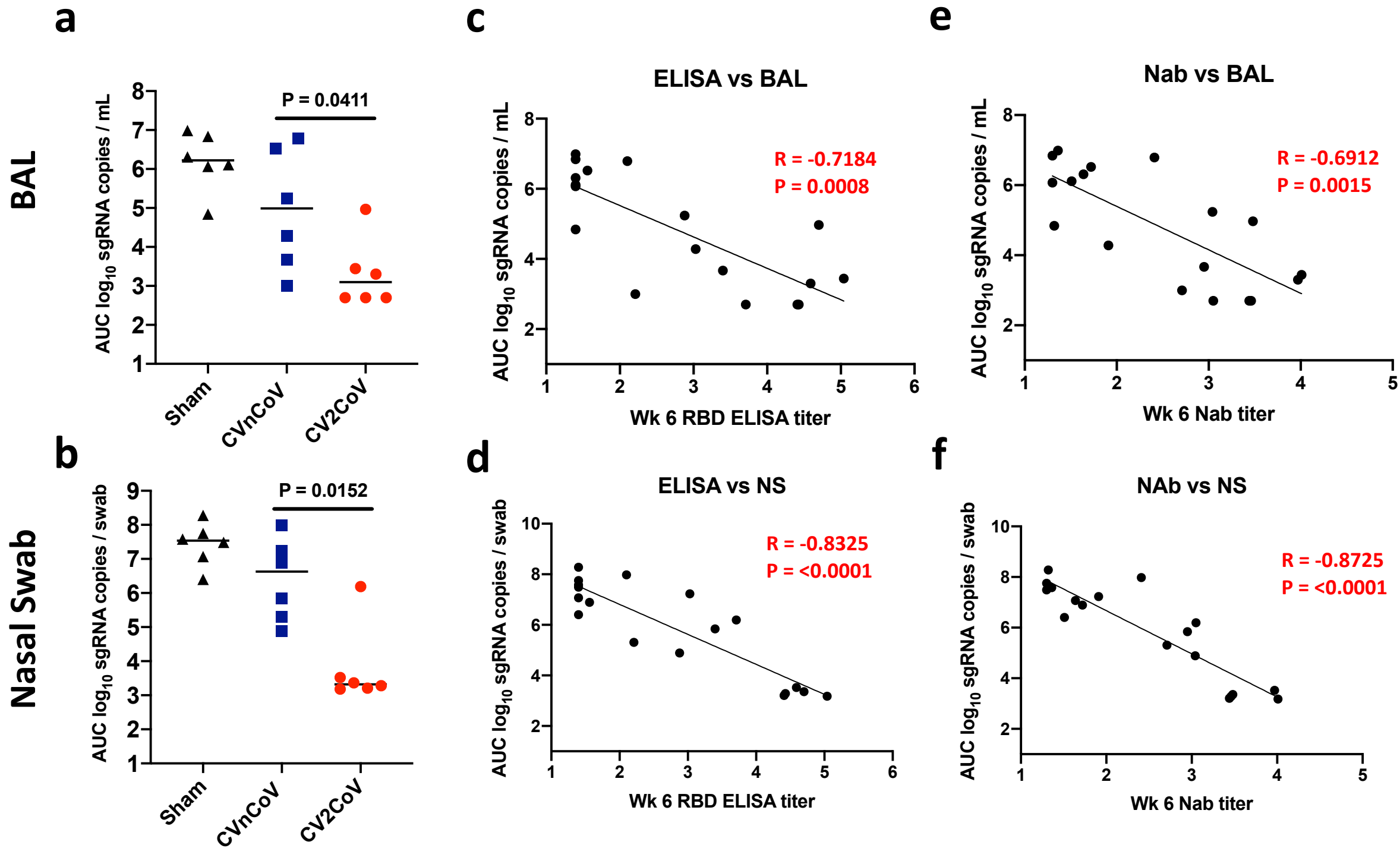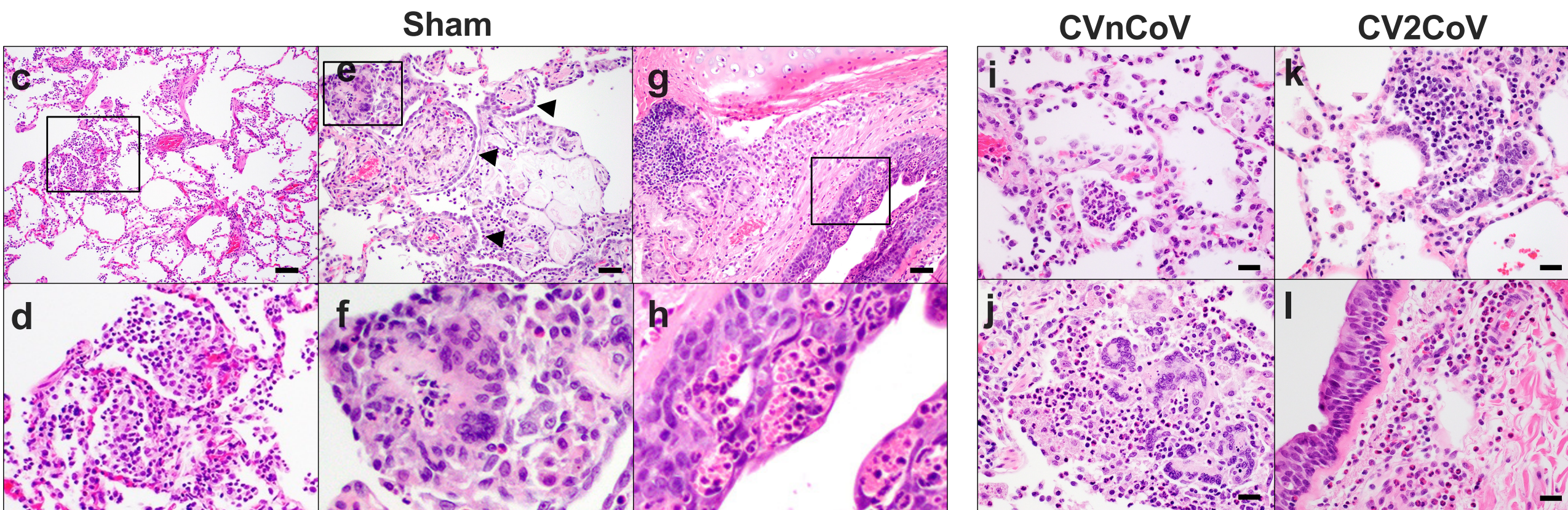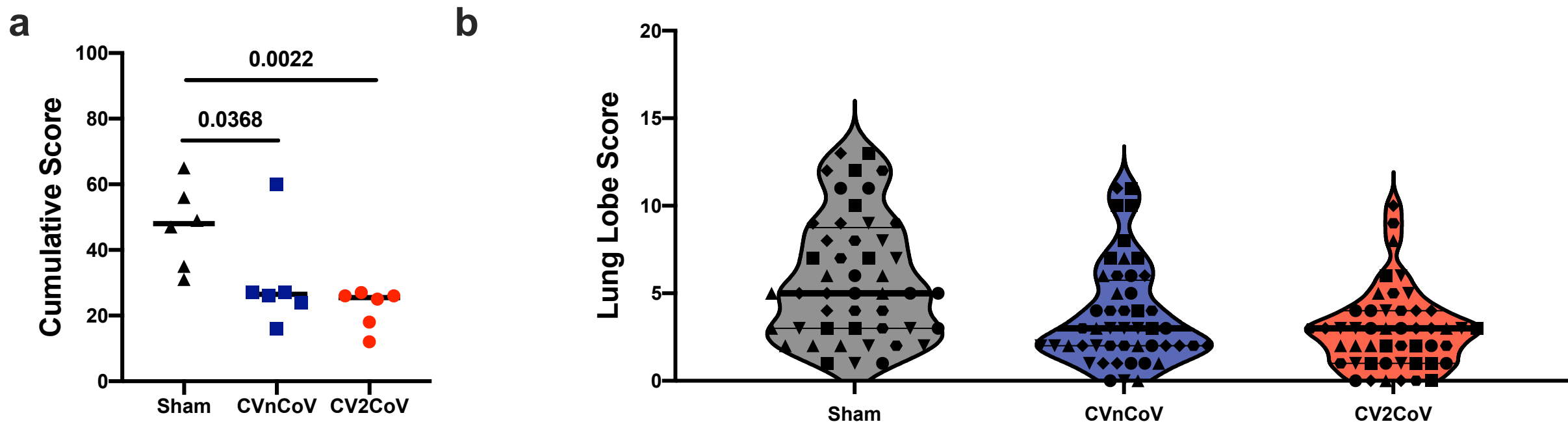Wk 6 NAb titer

Figure 5

Extended Data Figure 1
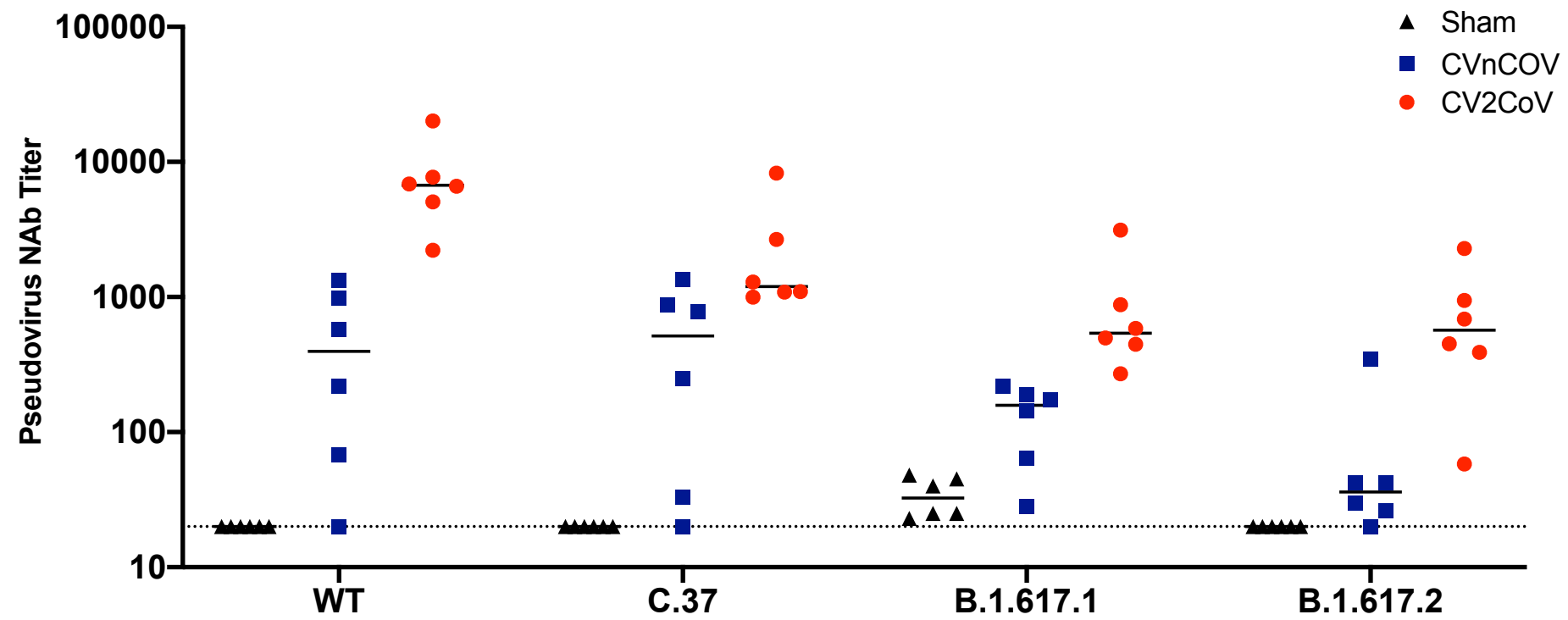
Extended Data Figure 2

Extended Data Figure 3

Extended Data Figure 4

Extended Data Figure 5